# Integration of 3D printed microlenses with vertically stacked photonic integrated circuits for biomedical applications

K. Obara*[a], C. Zhong[a], G. Osnabrugge[a], M. D. Sousa[a], T. Berns[a], N. Nijenhuis[a], M. Milosevic[a], A. S. Everhardt[b], F. Schreuder[b], A. M. Grammatikaki[c,d], M. Massaouti[c,d], H. Avramopoulos[c,d]
[a]PHIX Photonics Assembly, Hengelosestraat 525, 7521 AG Enschede, The Netherlands
[b]Lionix International, Hengelosestraat 500, 7521 AN Enschede, The Netherlands
[c]Institute of Communication and Computer Systems (ICCS), 42 Patission St., 10682 Athens, Greece
[d]National Technical University of Athens, 9 Iroon Polytechneiou, 15772 Zografou, Athens, Greece

## ABSTRACT

Analysis of extracellular vesicles (EVs) in blood samples is a key advancement of modern medicine allowing to diagnose conditions such as pancreatic cancer and cardiovascular disease. Photonic integrated circuits combined with 3D printed microlenses could be the heart of point-of-care medical devices optically detecting EVs as small as 150 nanometers in diameter. Within this paper we report on novel photonic device combining three photonic sensing methods: flow cytometry (FCM), fluorescence sensing and optical coherence tomography (OCT). The 3-in-1 multi-sensing platform is based on silicon nitride photonic integrated circuits (PIC), integrated with 3D printed microlenses as well as innovative photonic assembly techniques. Due to various operating wavelength ranges, the functions of FCM and fluorescence sensing (both 520 nm and 638 nm wavelengths) are combined on the same PIC, whereas the OCT functionality (750 nm–820 nm wavelength range) is realized on a separate PIC. After chip fabrication and lens 3D printing, both PICs get integrated through vertical stacking technique, resulting in enhanced device functionality and device miniaturization. Both PICs contain etched keyhole-shaped slots allowing for physical insertion and real-time active alignment of a medical glass capillary in their center. The transmitted and detected optical signals are propagating through free space (air). Microlenses get 3D printed on the internal circumference of the keyhole-shaped slots, focusing the light from the waveguides onto the glass capillary and collecting the scattered optical signal after its interaction with the biological sample. The additive manufacturing printing process combines two-photon polymerization with lithographic-level alignment technology. We report to have enabled high-precision printing of 3D microstructures with feature sizes down to 100 nanometers and optical-grade surface quality as well as their integration with vertically stacked photonic integrated circuits for biomedical applications such as FCM, fluorescence sensing and OCT.

**Keywords:** biomedical optics, lens 3d printing, photonic integrated circuit, extracellular vesicles, flow cytometry, fluorescence, optical coherence tomography

## 1. INTRODUCTION

Extracellular vesicles (EVs) are nanoscale particles in human blood, which have the potential for becoming biomarkers for detection of medical conditions such as pancreatic cancer and cardiovascular disease. At the same time, detection of EVs provides not only valuable information about the presence of the aforementioned diseases, but also about their progression and effectiveness of medical treatment, which makes EV analysis in blood samples one of the most promising advancements in modern medicine [1][2][3]. Photonic integrated circuits combined with 3D printed microlenses could be the heart of a compact point-of-care medical device optically detecting EVs as small as 150 nanometers in diameter. Such medical instrument would be realized in form of a 3-in-1 multi-sensing platform seamlessly integrating three different photonic sensing methods: flow cytometry (FCM), fluorescence sensing and optical coherence tomography (OCT) [4][5].

*k.obara@phix.com; phone +31 88 7449 000; phix.com

Integrated Optics: Devices, Materials, and Technologies XXX, edited by Sonia M. García-Blanco, Pavel Cheben,
Proc. of SPIE Vol. 13900, 1390008 · 2026 Published by SPIE
0277-786X · doi: 10.1117/12.3078100

## 2. METHODOLOGY

The discussed 3-in-1 multi-sensing platform is based on silicon nitride photonic integrated circuits (PIC), combined with 3D printed microlenses as well as equipped with innovative photonic assembly solutions.

The FCM and fluorescence subsystem is operated by using two wavelengths: 520 nm and 638 nm. Interaction between the optical signal and a biological sample propagating in the glass capillary results in emission of scattering and fluorescence signals, which are collected by waveguides distributed around the circumference of an etched keyhole-shaped slot at nine angular positions per wavelength – that being 0°, 20°, 40°, 60°, 80°, 100°, 120°, 140° and 160°. Each waveguide is terminated with a 3D printed microlens, in order to allow for efficient illumination of the biological channel and collection of the output optical signals, which afterwards get detected with the use of external avalanche photodiodes.

The OCT subsystem is operated in spectral domain, allowing creation of two one-dimensional imaging sections of the sensing area to identify the number of particles and estimate their position with respect to the horizontal plane. Waveguides representing the sample and reference arms of the subsystem are allocated around the circumference of the etched keyhole-shaped slot and are terminated with 3D printed microlenses. The OCT system operating wavelength range spans from 750 nm to 820 nm.

Due to various operating wavelength ranges (resulting in diverse thickness of silicon nitride waveguide layers) and an overlap in angular positions of the microlenses between both subsystems, the functions of FCM and fluorescence sensing are combined on the same PIC, whereas the OCT functionality is realized on a separate PIC. Both PICs contain etched keyhole-shaped slot fabricated via deep reactive-ion etching process, which allows for physical insertion and real-time active alignment of a medical-grade glass capillary in its center.

In order to terminate a waveguide with 3D printed microlens at a near-lithographic level of positioning accuracy, required is presence of specific alignment markers compatible with Nanoscribe Quantum x align vision recognition system. For this reason, a checker-square pattern constructed of counterchanged squares was deposited alongside the functional waveguide. At least two subsets (four copies) of counterchanged checker-square fiducials were embedded within the field-of-view of the microscope objective lens, in order to establish an XY-coordinate plane and to control an in-plane angular rotation during the 3D printing process. Both FCM/fluorescence and OCT subsystems utilized the same focusing microlens design, which was optimized for all operating wavelengths – 520 nm, 638 nm and 790 nm.

Both FCM/fluorescence PIC and OCT PIC were designed in a way to enable merging of the two individual subsystems together by implementing a dedicated assembly architecture, compatible allocation of all optical ports and incorporation of alignment fiducials in the silicon nitride waveguide layer to allow high accuracy vertical stacking of both PICs during the assembly phase. In such configuration, FCM/fluorescence PIC would serve as a motherboard, with the OCT PIC attached onto its top surface.

Eventually, the two PICs got vertically stacked to enable precise synchronization between the FCM, fluorescence sensing and OCT functionalities. Such integration scheme ensures efficient optical signal transmission and coordination between the modalities, enabling accurate and multimodal sample analysis within a compact photonic system.

## 3. EXPERIMENTAL RESULTS

Upon successful fabrication, the FCM/fluorescence and OCT PICs were assembled into a photonic module by using a combination of well-established techniques, such as optical edge-coupling and die bonding, as well as novel processes, like 3D printing of microlenses or vertical stacking of PICs. The complete assembly process flow consisted of numerous process steps, which were executed according to the following sequence:

1. Placement of the PICs onto submounts, in order to reinforce their mechanical structure through increasing the surface area-to-thickness ratio (aspect ratio).
2. Mechanical polishing of the facets, in order to obtain optical-grade surface flatness.
3. 3D printing of microlenses at the ends of waveguides by using two-photon polymerization (2PP) process.
4. Vertical stacking of both PICs with the use of high-accuracy die bonding process.
5. Optical assembly of fiber arrays with the FCM/fluorescence & OCT system through active alignment edge-coupling process.
6. Mechanical assembly of the FCM/fluorescence & OCT system onto a custom designed carrier baseplate with the use of die-attach process.

The study elaborating on the design, simulations and measurements of the 3D printed microlenses dedicated for light manipulation within the sensing PICs has been published separately [6]. The microlens measurement system consisted of a laser operating at a dedicated wavelength – 520 nm, 638 nm or 850 nm (measurement was realized at 850 nm, due to 790 nm wavelength light source unavailability), an attenuator, two fiber arrays equipped with a set of eight 3D printed microlenses and a photodetector. Both fiber arrays were positioned in front of one another and were separated by a distance of 2.54 mm, in order to emulate optical transmission conditions of the actual module. Optical signal from a laser was coupled through an attenuator to the connector of each fiber in an input array, whereas each fiber of an output array was connected to a photodetector. Subsequently, optical power emitted by each microlens of the input fiber array was set to 1.0 mW (0.0 dBm) with the use of an in-line attenuator. This value was measured by using a free-space optical power meter and served as a reference during the experiment. Characterization results of the microlenses revealed optical losses to be of the following average values: 0.41 dB at 520 nm wavelength, 0.47 dB at 638 nm wavelength, and 0.83 dB at 850 nm wavelength. Obtained measurement results correspond to coupling efficiencies of 91%, 90% and 83%, respectively. Figure 1 contains statistical analysis of experimentally measured optical losses for all 3D printed microlenses per operating wavelength.

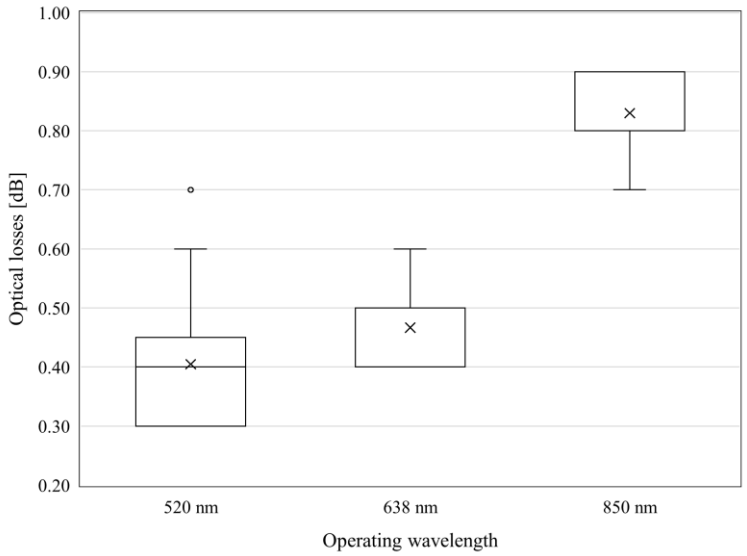


Figure 1. Statistical analysis of measured optical losses for 3D printed microlenses per operating wavelength. The lowest transmission losses were observed for 520 nm wavelength.

Before proceeding to 3D printing of microlenses on the FCM/fluorescence and OCT PICs, conducted was a lens shape optimization procedure, in order to establish and then minimize geometrical deviations between the optical design versus an actual geometry after 3D printing process. Examined were dimensional parameters like surface topography, radius

of curvature, diameter and height. The observed discrepancies were resulting from the factors of polymerization and shrinkage of the resin material during the two-photon polymerization (2PP) process.

Surface topography profile of a 3D printed microlens after shape optimization procedure was obtained with the use of a confocal microscope and is presented in Figure 2. As a result of the microlens shape optimization procedure, it was determined that the surface topography differences between the optical design and an actual 3D printed geometry are on the order of less than λ/8 over 80%+ of the lens surface area for operating wavelength range of 750–820 nm and less than λ/5 over 80%+ of the lens surface area for an operating wavelength of 520 nm. Post-process parameters of microlens height and radius got adjusted to fit within 1% tolerance range compared to the optical design.

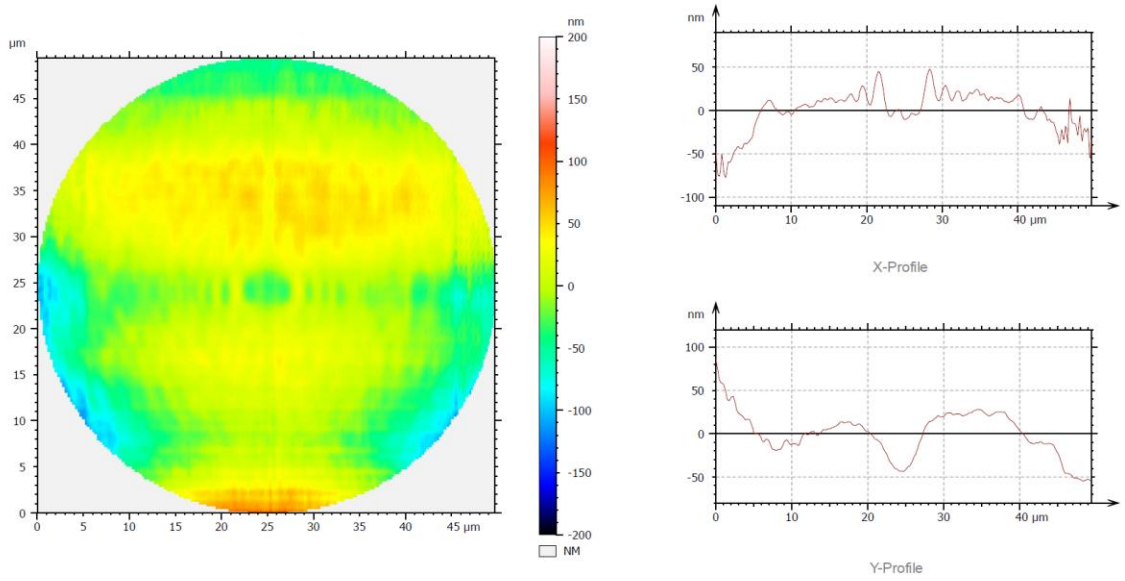


Figure 2. Surface topography profile of a 3D printed microlens after shape optimization procedure, showing surface flatness on the order of less than λ/8 over 80%+ of the lens surface area for operating wavelength range of 750–820 nm and less than λ/5 over 80%+ of the lens surface area for an operating wavelength of 520 nm.

As explained in the methodology section, both PICs contain etched keyhole-shaped slots, which allow physical insertion and real-time active alignment of a medical-grade glass capillary in their center. Each waveguide got terminated with a 3D printed microlens within the area of an etched slot, in order to allow for efficient illumination of the biological channel and collection of the output optical signals. To enable this functionality, employed was an additive manufacturing process combining two-photon polymerization (2PP) with a state-of-the-art visual alignment technology. Harnessing of Nanoscribe Quantum x align system capabilities with Nanoscribe IP-S photoresin resulted in obtaining 3D printed microstructures with feature sizes down to 100 nanometers and optical-grade surface quality. Near-lithographic positioning accuracy of the 3D printed microlenses was achieved thanks to including a set of alignment markers in the waveguide layer. Twenty-two units (in case of the FCM/fluorescence PIC) and four units (in case of the OCT PIC) of focusing microlenses got successfully 3D printed at the ends of waveguides allocated within the etched keyhole-shaped slots of both PICs. Results of the two-photon polymerization microfabrication process are shown in Figure 3a and Figure 3b.

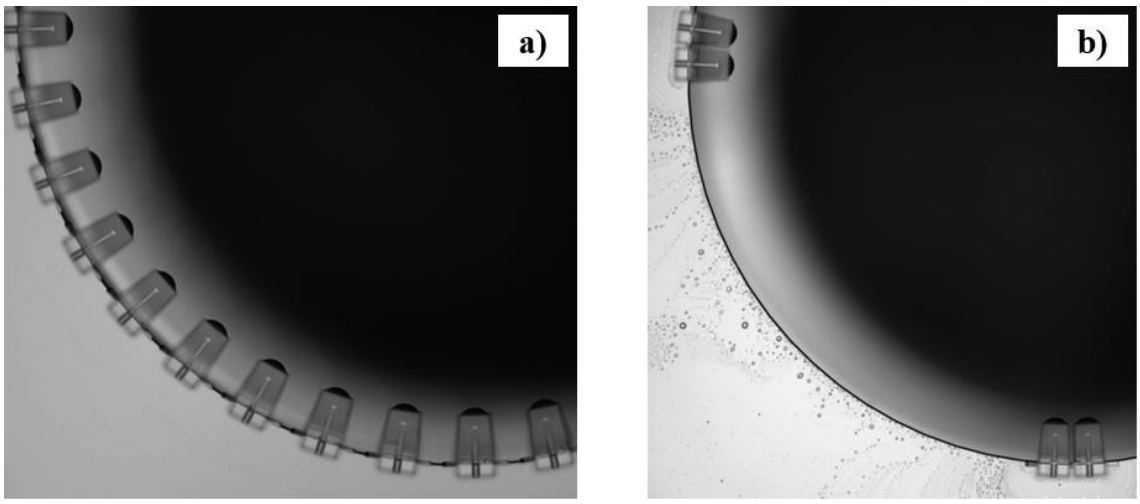


Figure 3. Focusing microlenses 3D printed at the ends of waveguides allocated within the etched keyhole-shaped slots of both PICs: a) FCM/fluorescence PIC, b) OCT PIC. Microlenses were printed with near-lithographic positioning accuracy and exhibited feature sizes down to 100 nanometers with optical-grade surface quality.

Edge-coupler waveguide terminations allocated at the input/output optical facets of both FCM/fluorescence and OCT PICs were fabricated in a silicon nitride layer structured to provide an optimal overlap with gaussian beam profiles of optical fibers at given operating wavelengths. Selected were single-mode optical fibers characterized with 3.5 ± 0.3 µm mode-field diameter at 460 nm wavelength (FCM/fluorescence application) and 4.5 ± 0.5 µm mode-field diameter at 630 nm wavelength (OCT application). Optical coupling losses at the fiber-PIC interface were determined through fiber-in/fiber-out measurements of test structures, which contained numerous straight waveguides of varying width. Measurement setup consisted of a supercontinuum white light laser source, two units of PM-S405-XP fibers (FCM/fluorescence PIC) or PM630-HP fibers (OCT PIC) and an optical spectrum analyzer. The system was first calibrated and normalized through active alignment between the physically contacted fibers of the same type. Subsequently, the insertion loss coming from the PIC introduced in-line was determined by aligning the first fiber to the input channel (west facet) and the second fiber to the output channel (east facet). Acquired numerical data was divided by a factor of two, in order to provide losses per single interface. Characterization results of the optical transition losses at the fiber-PIC interface are shown in Figure 4a and Figure 4b. In case of the FCM/fluorescence PIC, the losses equal to 3.2 dB per facet at 520 nm wavelength and 1.5 dB per facet at 638 nm wavelength. For the OCT PIC, the loss equals to 1.5 dB per facet at 800 nm wavelength.

Additionally, with the use of a previously described fiber-in/fiber-out measurement system, established were optical propagation losses in waveguides of both FCM/fluorescence and OCT PICs. For this purpose, fabricated test PICs got equipped with spiral-shaped waveguides. Optical propagation loss measurements as a function of wavelength for both FCM/fluorescence and OCT PICs are shown in Figure 5a and Figure 5b. Characterization results reveal a strong correlation with operating wavelength due to longer wavelengths exhibiting less scattering. At the same time, the measurement results show a strong relationship with light confinement within the waveguide structure. The larger the confinement, the higher the propagation losses, but also the smaller the allowed bend radius and mode-field diameter value. Waveguides of the FCM/fluorescence PIC were designed to have low light confinement, which resulted in low propagation loss of 0.22 dB/cm at 520 nm wavelength and 0.09 dB/cm at 638 nm wavelength. On the other hand, waveguides of the OCT PIC have high confinement, and therefore revealed a high propagation loss of 0.37 dB/cm at 800 nm wavelength. Nonetheless, all measured propagation loss values are acceptable for the biomedical applications, due to total travel distance of optical signals being limited to less than a few centimeters.

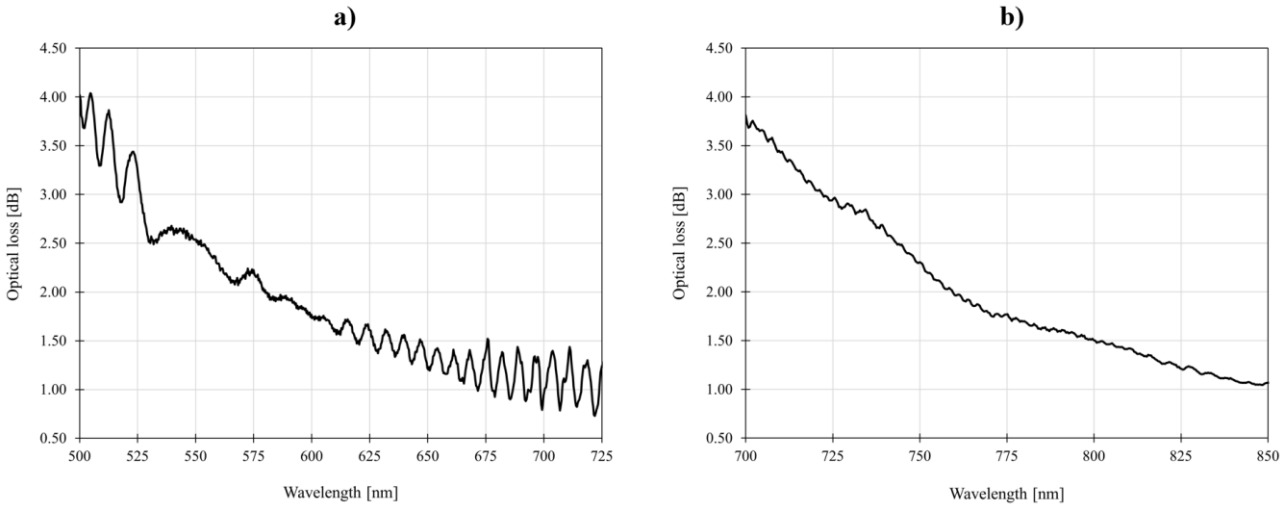


Figure 4. Optical transition losses at the fiber-PIC interface measured for: a) FCM/fluorescence PIC, b) OCT PIC. In case of the FCM/fluorescence PIC, the losses equal to 3.2 dB per facet at 520 nm wavelength and 1.5 dB per facet at 638 nm wavelength. For the OCT PIC, the loss is 1.5 dB per facet at 800 nm wavelength.

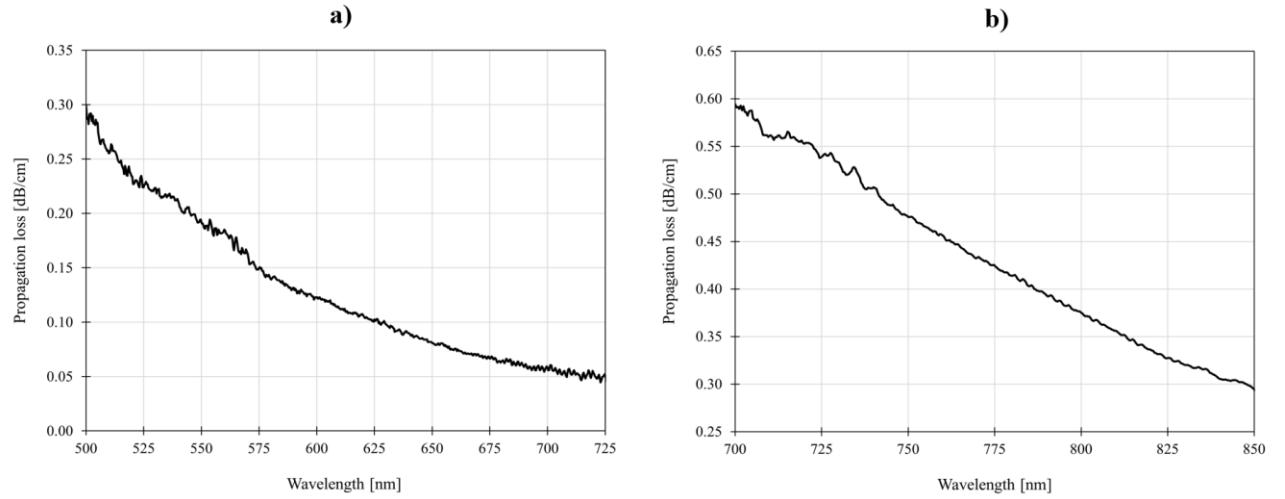


Figure 5. Optical propagation loss as a function of wavelength for: a) FCM/fluorescence PIC, b) OCT PIC. Waveguides of the FCM/fluorescence PIC exhibited low propagation loss of 0.22 dB/cm at 520 nm wavelength and 0.09 dB/cm at 638 nm wavelength due to low confinement. Waveguides of the OCT PIC exhibited higher propagation loss of 0.37 dB/cm at 800 nm wavelength due to high confinement.

The discussed PICs got attached in a vertically stacked configuration, with their waveguide layers oppositely allocated, to reduce the travel distance of the biological sample between the analysis stages of the FCM/fluorescence and the OCT. Glass spacer slotted between both PICs was designed to prevent inducing mechanical damage to the 3D printed microlenses through manipulation of the capillary, i.e. as a result of a collision. Vertical stacking of the PICs was realized with the use of Finetech FINEPLACER femto 2 die bonding system, which allowed placement accuracy within ±5 µm range, thanks to including a set of on-chip alignment fiducials in the waveguide layer.

Subsequently, three fiber arrays were optically edge-coupled to the vertically stacked FCM/fluorescence & OCT PICs with the use of an active alignment procedure, to serve a purpose of input-illumination and output-coupling for scattering and fluorescence optical signals. The fiber array responsible for guiding input-illumination at 520 nm and 638 nm wavelengths was integrated using a technique allowing handling of elevated optical power level without degradation in parameters of transmittance and lifetime of the optical adhesive joining the two interfaces. Eventually, the discussed photonic assembly was mounted onto a custom designed carrier baseplate to assure its stability and robustness. Presented hybrid integration approach enabled co-packaging of the FCM, fluorescence sensing and OCT modalities within a single, miniaturized system. Photonic assembly of vertically stacked FCM/fluorescence & OCT PICs is shown in Figure 6. In Figure 7. presented is a detailed view into the area where the 3D printed microlenses are allocated within the etched keyhole-shaped slots of both vertically stacked PICs.

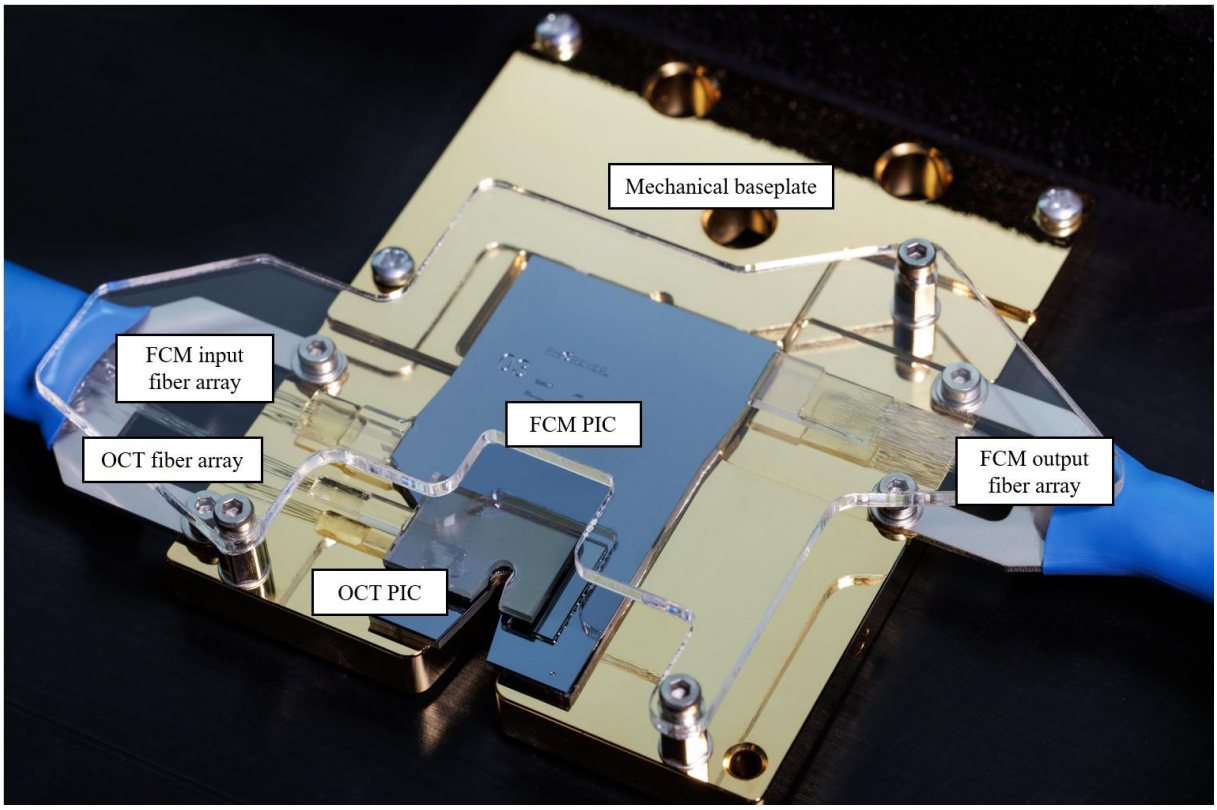


Figure. 6. Photonic assembly of vertically stacked FCM/fluorescence & OCT PICs.

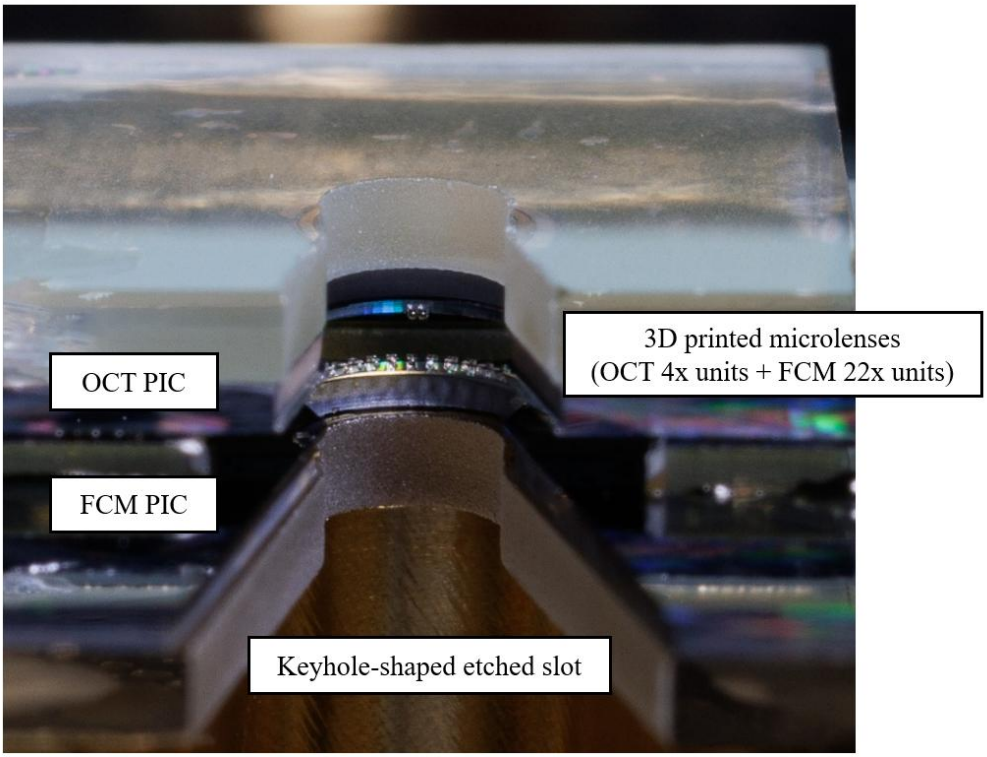


Figure. 7. Detailed view into the area of vertically stacked FCM/fluorescence & OCT PICs, where the 3D printed microlenses are allocated around the keyhole-shaped etched slot.

## 4. SUMMARY

We report to have successfully designed, fabricated and assembled a 3-in-1 multi-sensing platform dedicated to analysis of extracellular vesicles (EVs) in blood samples based on silicon nitride photonic integrated circuits (PIC). This achievement comes as a result of definition, development and implementation of novel integration techniques, like two-photon polymerization 3D printing, microlens shape optimization procedure as well as vertical stacking of PICs. Optical transition losses at the fiber array-PIC interface equal to 3.2 dB per facet at 520 nm wavelength, 1.5 dB per facet at 638 nm wavelength and 1.5 dB per facet at 800 nm wavelength. Optical propagation losses equal to 0.22 dB/cm at 520 nm wavelength, 0.09 dB/cm at 638 nm wavelength and 0.37 dB/cm at 800 nm wavelength. Successful implementation of microlens shape optimization procedure resulted in reduction of geometrical deviations between the optical design and actual 3D printed geometry with regards to dimensional parameters of surface topography, radius of curvature, diameter and height. Twenty-two units (in case of the FCM/fluorescence PIC) and four units (in case of the OCT PIC) of focusing microlenses were 3D printed at the ends of waveguides allocated around the etched keyhole-shaped slots with the use of two-photon polymerization process. All microlenses exhibited feature sizes down to 100 nanometers, optical-grade surface quality and lithographic-level alignment thanks to including dedicated fiducials in the waveguide layer. The FCM/fluorescence and OCT PICs were attached in a vertically stacked configuration with placement accuracy within ±5 μm range, which enabled precise synchronization between all functionalities. The hybrid photonic integration approach discussed in this paper enabled successful co-packaging of the FCM, fluorescence sensing and OCT modalities within a single, miniaturized system aiming at optical detection of EVs as small as 150 nanometers in diameter. Technical validation and performance analysis of the assembled 3-in-1 multi-sensing platform will be published as a separate study.

## ACKNOWLEDGEMENTS

This work is a part of the PHOREVER project. This project has received funding from the European Union's Horizon 2022 research and innovation program under grant agreement No. 101093171. Content reflects only the authors' view, and the Research Executive Agency (REA) / European Commission is not responsible for any use that may be made of the information it contains.

## REFERENCES

[1] E. J. Benjamin et al., "Heart Disease and Stroke Statistics-2019 Update: A Report From the American Heart Association," 139(10), Circulation, e56–e528 (2019); https://doi.org/10.1161/CIR.0000000000000659

[2] H. A. Wafa et al., "Burden of Stroke in Europe: Thirty-Year Projections of Incidence, Prevalence, Deaths, and Disability-Adjusted Life Years," 51(8), Stroke, 2418–2427 (2020); https://doi.org/10.1161/STROKEAHA.120.029606

[3] A. D. Singhi et al., "Early Detection of Pancreatic Cancer: Opportunities and Challenges," 156(7), Gastroenterology, 2024–2040 (2019); https://doi.org/10.1053/j.gastro.2019.01.259

[4] K. Wörhoff et al., "TriPleX: A Versatile Dielectric Photonic Platform," 4(2), Advanced Optical Technologies, 189–207 (2015); https://doi.org/10.1515/aot-2015-0016

[5] J. Botha et al., "Conventional, High-Resolution and Imaging Flow Cytometry: Benchmarking Performance in Characterisation of Extracellular Vesicles," 9(2), Biomedicines, 124 (2021); https://doi.org/10.3390/biomedicines9020124

[6] A.M. Grammatikaki et al., "Development of 3D-printed microlenses at the edge of waveguides of flow cytometry and optical coherence tomography photonic integrated circuits", Proc. SPIE 13369, Integrated Optics: Devices, Materials, and Technologies XXIX, 133690V (19 March 2025); https://doi.org/10.1117/12.3042890